New Phytologist

Research

Medullary bundles in Caryophyllales: form, function, and evolution

Israel L. Cunha Neto[1,2], Elson Felipe S. Rossetto[3], Caian S. Gerolamo[2], Rebeca Hernández-Gutiérrez[4], Alexander P. Sukhorukov[5,6], Maria Kushunina[6,7], Gladys F. A. Melo-de-Pinna[2] and Veronica Angyalossy[2]

[1]Department of Environmental Studies, New York University, New York, NY 10012, USA; [2]Department of Botany, Institute of Biosciences, University of São Paulo, Cidade Universitária, São Paulo, SP, 05508-090, Brazil; [3]Department of Animal and Plant Biology, Center of Biological Sciences, State University of Londrina, Campus Universitário, Londrina, PR, 86057-970, Brazil; [4]Department of Evolution, Ecology, and Organismal Biology, University of California, Riverside, CA 92521, USA; [5]Department of Higher Plants, Biological Faculty, M.V. Lomonosov Moscow State University, Moscow, 119234, Russia; [6]Laboratory Herbarium (TK), Tomsk State University, Tomsk, 634050, Russia; [7]Department of Plant Physiology, Biological Faculty, M.V. Lomonosov Moscow State University, Moscow, 119234, Russia

Author for correspondence:
Israel L. Cunha Neto
Email: israellopescn@gmail.com

Received: *6 April 2023*
Accepted: *2 October 2023*

New Phytologist (2024) **241:** 2589–2605
doi: 10.1111/nph.19342

Key words: Cactaceae, evolution of correlated traits, hydraulic conductivity, medullary bundles, state-dependent diversification, trait evolution, vascular tissue.

Summary

- The occurrence of conducting vascular tissue in the pith (CVTP) of tracheophytes is noteworthy. Medullary bundles, one of the remarkable examples of CVTP, evolved multiple times across angiosperms, notably in the Caryophyllales. Yet, information on the occurrence of medullary bundles is fragmented, hampering our understanding of their structure–function relationships, and evolutionary implications.
- Using three plastid molecular markers (*matK*, *rbcL*, and *rps16 intron*), a phylogeny is constructed for 561 species of Caryophyllales, and anatomical data are assembled for 856 species across 40 families to investigate the diversity of medullary bundles, their function, evolution, and diversification dynamics. Additionally, correlated evolution between medullary bundles and successive cambia was tested.
- Medullary bundles are ancestrally absent in Caryophyllales and evolved in core and noncore families. They are structurally diverse (e.g. number, arrangement, and types of bundles) and functionally active throughout the plant's lifespan, providing increased hydraulic conductivity, especially in herbaceous plants. Acquisition of medullary bundles does not explain diversification rate heterogeneity but is correlated to a higher diversification rate.
- Disparate developmental pathways were found leading to rampant convergent evolution of CVTP in Caryophyllales. These findings indicate the diversification of medullary bundles and vascular tissues as another central theme for functional and comparative molecular studies in Caryophyllales.

Introduction

The organization of vascular bundles and associated tissues in the primary plant axis, that is the stele, is a fundamental concept in plant biology (Beck *et al.*, 1982; Tomescu, 2021). As distinct types of stele organizations appear through evolutionary time, the eustele – a ring of vascular bundles surrounding the pith – evolved within lignophytes (Decombeix *et al.*, 2019). They now characterize the stems of most extant seed plants (Tomescu, 2021). Modifications to this eustele occur at distinct levels; the 'atactostele' of monocots (Beck *et al.*, 1982) and the 'polycyclic eustele' (Beck *et al.*, 1982), which consist of vascular bundles, called medullary bundles, occupying the pith in nonmonocot lineages (De Bary, 1884; Philipson & Balfour, 1963). Medullary bundles evolved multiple times across the tracheophytes characterizing polycyclic dictyosteles, siphonosteles, or solenosteles in ferns (Suissa & Friedman, 2022) and the polycyclic eusteles in seed plants, which have been reported in gymnosperms (e.g. cycads) and angiosperms (Beck *et al.*, 1982; Isnard *et al.*, 2012). The medullary bundles of angiosperms evolved independently in several lineages with occurrences across the magnoliids (e.g. Piperales) and eudicots, including rosids (e.g. Myrtales), asterids (e.g. Apiales), and remarkably in the diverse order Caryophyllales (Gibson, 1994).

Caryophyllales is a relatively large lineage of flowering plants with > 12 500 species (Hernández-Ledesma *et al.*, 2015). The order comprises economically important species (e.g. beets and quinoa) and is distinguished by the repeated evolution of unusual ecological adaptations, including succulents, gypsophilous and carnivorous plants (Hernández-Ledesma *et al.*, 2015; Walker *et al.*, 2018). Some Caryophyllales also contain betalain pigments instead of anthocyanin (Brockington *et al.*, 2015; Timoneda

et al., 2019), have unique flower development (Brockington *et al.*, 2009; Ronse de Craene, 2021), diverse fruit types (Sukhorukov *et al.*, 2015), and vascular variants (Cunha Neto, 2023), markedly the anatomical pattern called successive cambia (Carlquist, 2010; Timonin, 2011). Also considered as a procambial variant (Cunha Neto, 2023), medullary bundles are another striking anatomical feature in the vascular system of Caryophyllales. They occur in many charismatic plants of Cactaceae (cacti), Droseraceae (sundews), Nepenthaceae (pitcher plants), and Nyctaginaceae (4 o'clock; DeBuhr, 1977; Mauseth, 1993; Schwallier *et al.*, 2017; Cunha Neto *et al.*, 2020a). These lineages encompass plants with diverse growth forms and habitats, representing an excellent group to investigate the form, function, and evolution of medullary bundles on a broad scale.

Medullary bundles are not restricted phylogenetically to closely related groups of Caryophyllales; therefore, their evolution is most likely homoplastic. In noncore Caryophyllales, medullary bundles seem to be poorly represented with only a few species possessing these structures (e.g. Droseraceae: DeBuhr, 1977; Nepenthaceae: Schwallier *et al.*, 2017). In contrast, they are pervasive in Amaranthaceae *sensu stricto*, Cactaceae, and other families within core Caryophyllales. In the family Cactaceae, medullary bundles can be found in several members of the Cactoideae but are absent in other subfamilies (Mauseth, 1993; Terrazas & Arias, 2002; Soffiatti & Angyalossy, 2007; Arruda & Melo-De-Pinna, 2010). Due to the lack of medullary bundles in lineages that are sister to the rest of the family (e.g. *Pereskia*), they are hypothesized to be ancestrally absent in the family (Mauseth, 1993). In contrast, medullary bundles are ubiquitous throughout the Nyctaginaceae, absent only in the tribe Leucastereae (Cunha Neto *et al.*, 2020a), and are present also in closely related families of the phytolaccoid clade (e.g. Phytolaccaceae: Kirchoff & Fahn, 1984). Within this clade, the acquisition of medullary bundles (but not the evolution of the climbing habit) is associated with increased diversification rates (Cunha Neto *et al.*, 2022). The broad phylogenetic distribution of medullary bundles and the remarkable ecological diversity of Caryophyllales species make this a captivating group for studying the evolutionary impact of medullary bundles in a broad-scale analysis.

Anatomical evidence suggests that medullary bundles remain functional even in mature stems (Mauseth, 1993; Cunha Neto *et al.*, 2020a). This includes vascular bundles formed at early development in plants estimated to be 150 yr old, which contain > 200 bundles in a single cross-section and continue to be metabolically active in conduction (e.g. saguaro cactus; Macdougal, 1926; Gibson & Nobel, 1986). This evidence supports the hypothesis that the appearance of medullary bundles is associated with the evolution of large pith of columnar cacti, which facilitate sugar and water transport to and from the pith and to the vascular system (Gibson & Nobel, 1986; Terrazas Salgado & Mauseth, 2002). Moreover, medullary bundles have been associated with other physiological demands, including starch storage and hydraulic conductivity in plants that produce numerous seeds or 'that hibernate by means of tuber and rhizome' (Haberlandt, 1914). However, there is currently a lack of functional studies that demonstrate the physiological significance of medullary bundles, which highlights the need for further investigation and deeper understanding in this critical area.

Here, we explored anatomical data within a phylogenetic framework in order to: (1) investigate the structural diversity of medullary bundles across the Caryophyllales; (2) reconstruct the evolutionary history of medullary bundles; (3) understand whether lineages with medullary bundles have higher diversification rate when compared to lineages without them; and (4) assess the form and function relationships of medullary bundles in species with distinct growth habits.

Materials and Methods

Taxon sampling

To obtain information on the presence and absence of medullary bundles, we collected stem samples of plants in the field or specimens from herbaria and wood collections (Supporting Information Table S1). Anatomical data were also obtained from publications that clearly addressed medullary bundles (Methods S1). The anatomical samples were combined with published data to build the largest dataset on the presence of medullary bundles to date (Table S1). In total, our dataset comprised 856 taxa distributed across 316 genera, from 40 families of Caryophyllales (Table S1). Scientific names were updated following Hernández-Ledesma *et al.* (2015) or the Plants of the World Online database (KEW; https://powo.science.kew.org/).

Anatomical studies

In addition to species of the phytolaccoid clade recently studied (Cunha Neto *et al.*, 2020a), other species with and without medullary bundles were investigated to obtain developmental information: Amaranthaceae: *Alternanthera brasiliana* (L.) Kuntze, *Chamissoa altissima* (Jacq.) Kunth; Petiveriaceae: *Gallesia integrifolia* (Spreng.) Harms; and Phytolaccaceae: *Phytolacca thyrsiflora* Fenzl ex J.A. Schmidt. To that aim, we performed anatomical studies of stems at different developmental stages (Methods S1). For the remaining collected species (Table S1), one or two stages were studied for the presence/absence of medullary bundles.

Phylogenetic analyses and tree topology

The molecular dataset was built from GenBank sequences for three plastid markers (*matK*, *rbcL* and *rps16* intron) of taxa included in the anatomical dataset (Table S1). For some taxa with anatomical information only at the genus level (e.g. 21 cases within Cactaceae), we added one species to represent that genus in the phylogeny. Similarly, in cases where sequences were not available for the species listed in Table S1, we included sequences of other species from the same genus (e.g. *Asteropeia* Thouars). The final dataset comprised 561 taxa (560 species and one variety), representing 270 genera and 40 families of Caryophyllales (Tables S1, S2). For outgroups, we selected two species representing the orders Ericales and Zygophyllales.

Sequences were aligned using ClustalW (Thompson *et al.*, 1994) as implemented in BioEdit v.7.2.5 (Hall, 1999) and checked using Mesquite v.3.61 (Maddison & Maddison, 2019). For each locus, the nucleotide substitution model was selected under Akaike Information Criterion (AIC) through PartitionFinder program v.2.1.1 (Lanfear *et al.*, 2012). Gaps were treated as missing data. To check incongruences among gene trees, individual maximum likelihood (ML) trees were estimated for each marker using RAxML v.8 (Stamatakis, 2014), under the GTRGAMMA model and 1000 runs of rapid bootstraps. Gene trees of each marker showed to be similar at the family level (Methods S2).

For ancestral state reconstruction and diversification analyses, we estimated divergence times using fossil information to calibrate the tree in a Bayesian framework implemented in Beast v.2.6.7 (Bouckaert *et al.*, 2019). We used the same combined molecular matrix as described previously (*matK*, *rbcL*, and *rps16* intron) and set the uncorrelated relaxed molecular clock model with lognormal distribution (UCLN model; Drummond *et al.*, 2006) and the birth–death model of tree reconstruction. We applied six calibration points. For the node of crown Caryophyllales, we applied a secondary calibration following Yao *et al.* (2019), who argued that the penalized likelihood was preferable than the Bayesian time tree; thus, we used a normal distribution with mean 114.4 and 0.5 set for the sigma parameter, which covers the credibility interval of the age estimated by Yao *et al.* (2019). The rest of the calibrations are based on the fossil record, using a uniform distribution with the minimum age derived from the minimum stratigraphic age of each fossil, and the maximum age corresponding to the mean age of crown Caryophyllales (i.e. 114.4 Ma). We ran two independent analyses, each with 300 million generations, sampling parameters every 10 000 generations. We corroborated the convergence of the Markovian chains if the Effective Sample Size was 200 or higher using Tracer v.1.6 (Rambaut *et al.*, 2014). Finally, a maximum clade credibility (MCC) tree was annotated from the posterior distribution with a 45% burn-in (see Dataset S1; Methods S3 for phylogeny and Dataset S2 for dated phylogeny).

Ancestral character state reconstruction and tests of correlated evolution

To evaluate the tempo, mode, and phylogenetic signal of the evolution of medullary bundles in Caryophyllales, we compared transformation models for this character. We evaluated the models of lambda (λ), delta (δ), and kappa (κ; Pagel, 1999), early burst models (EB; Blomberg *et al.*, 2003) and the rate constancy through time model (none) were compared with the value obtained from the nonphylogenetic (white noise) model. Then, the evolution of medullary bundles was estimated through Bayesian stochastic mapping (Bollback, 2006) on the MCC tree. Character states were coded as (0) typical eustele (medullary bundles absent) and (1) polycyclic eustele (medullary bundles present; Table S3). Model fit was selected among equal rates (ER), symmetric (SYM), and all rates different (ARD). To assess the best-fit model for both transformation and transition models (Table S4), we used the AIC in the function *fitDiscrete* of the R package Geiger (Pennell *et al.*, 2014). Posterior probabilities of ancestral character states were plotted at tree nodes after 1000 simulations of stochastic mapping through the *make.simmap* function of the R package Phytools (Revell, 2012). The function *countsimmap* was used to summarize mean and standard deviation of transitions between the states.

Correlated evolution of medullary bundles and successive cambia was tested using the Pagel's (1994) method implemented in the *fit.pagel* function of Phytools, under the best-fit model ER. For this analysis, the phylogeny used in the ancestral character state reconstruction (ASR) analysis was trimmed to match the successive cambia dataset. The presence/absence of successive cambia was coded following Carlquist (2010) and references therein. Other data were included from other sources to include representatives of newly delimited families (Dataset S3). All analyses were performed using R v.4.1.3 (R Core Team, 2022).

Diversification rate estimation

We aimed to test whether the diversification rate of Caryophyllales has been heterogeneous through time and among clades. We used two methods for this analysis, a Bayesian and a maximum likelihood approach. The Bayesian method was implemented in BAMM (Rabosky, 2014). For the maximum likelihood, we used the R package MEDUSA (Alfaro *et al.*, 2009). We performed both approaches because it has been argued that MEDUSA is more appropriate than BAMM for incomplete phylogenies that represent high-rank taxonomic groups (Rabosky, 2018). For the analysis with BAMM, we first set up the priors adequate for our dataset with BAMMtools (Rabosky *et al.*, 2014). We incorporated a list of species and the proportion of species sampled for each genus and for genera not included in our phylogeny (Table S3). We ran BAMM for 10 million generations, sampling every 1000 generations. We corroborated the convergence of Markov chains with coda (Plummer *et al.*, 2006). For MEDUSA, we also considered incomplete taxon sampling, and we tested two modes of diversification, one through speciation only, and the other considering both speciation and extinction.

Diversification analyses showed numerous diversification rate shifts; thus, the second step was to explore whether the medullary bundles can explain these rate shifts. We used the Hidden State Speciation and Extinction (HiSSE) method (Beaulieu & O'Meara, 2016) that allows us to test the relative contribution of an observed trait (i.e. the presence of medullary bundles) to the diversification rate. We estimated rates of turnover (τ) and state transition (q) testing five models. Each model represents a hypothesis about the dynamics of the diversification and the evolution of medullary bundles. For the extinction fraction parameter (ε), we allowed only one rate for all states in each model. In the first model (Null), the diversification rates do not change in the phylogeny. In the second model, diversification rates are allowed to vary in accordance with the observed character (BiSSE-like model). The third model considers the possibility that an unobserved trait (i.e. a hidden trait with two states, A and B) better explains the diversification rate heterogeneity (HiSSE model). Then, we included two models of trait-independent

diversification. One in which the turnover rate is the same for the states of each type of trait (observed and hidden), and the other one is similar but with two additional states. To assess the impact of missing taxa, we ran two series of analyses of the five models, one considering that our taxon sampling was complete, and the other considering missing taxa.

We used AIC to select the model that best describes our data. Additionally, we examined whether there are significant differences in diversification rates between the species with the absence or presence of medullary bundles using the function GetModelAveRates in the HiSSE package.

Function and contribution of medullary bundles to hydraulic conductivity

To investigate the hydraulic conductivity of medullary bundles, we performed two experiments using four species from Nyctaginaceae with distinct habits: *Allionia incarnata* L. (perennial herb), *Bougainvillea spectabilis* Willd. (shrubby liana), *Mirabilis jalapa* L. (perennial herb), and *Pisoniella glabrata* (Heimerl) Standl. (shrubby liana). *Allionia* and *Mirabilis* are considered 'herbaceous', or plants with limited amounts of wood, and *Bougainvillea* and *Pisoniella* are considered woody shrubby lianas with considerable amounts of wood. *Experiment 1*: aimed at investigating whether medullary bundles are functionally conducting water. To that aim, we selected three integral branches (with leaves) of *Bougainvillea spectabilis* and *Mirabilis jalapa*, cut the base of each branch under water, and attached a tube with safranin dye diluted in water (0.05% concentration) to let the branches transpire for 24 h. The dye travels preferentially through vessels that are conductive and stains their cell walls, marking them as functional in the water flow of an intact transpiring plant. After 24 h, we cut the stem from bottom to top into 5-mm-long pieces and made freehand sections to assess which tissues were functional and how far they reached in the stem (Figs S1, S2; Zimmermann & Jeje, 1981). *Experiment 2*: aimed at investigating the contribution of medullary bundles and secondary xylem to the total potential hydraulic conductivity in three developmental stages. Plants with different habits and arrangements of medullary bundles were used: *Allionia incarnata* (one ring with eight medullary bundles), *Pisoniella glabrata* (> 10 concentric rings of medullary bundles), and *Mirabilis jalapa* (> 10 concentric rings of medullary bundles). Three individuals of each species were evaluated. Cross sections of stems during primary growth (near the apex), transition from primary to secondary growth (internodes below the shoot apex), and mature stems of each individual were analyzed to calculate area of vessels in both medullary bundles and secondary xylem. All measures were performed using ImageJ, v.1.45d (http://rsb.info.nih.gov/ij/). Area of each vessel was converted to vessel diameter using the equation: $D = 2 \times \sqrt{\text{area}/\pi}$; and with the vessel diameter of all vessels in each cross section of each individual, we calculated the potential hydraulic conductivity (Kp) for both medullary bundles and secondary xylem using the equation: $Kp = (\pi pw/128\eta) \times \Sigma D^4$, following Hagen–Poiseuille's law (Tyree & Ewers, 1991), where Kp is the potential hydraulic conductivity (kg m Mpa^{-1} s^{-1}), pw is the density of water at 20°C (998.2 kg m^{-3}), η is the water viscosity at 20°C (1.002×10^{-3} Pa s^{-1}), and D is vessel diameter (m).

The total potential conductivity was calculated as the sum of the potential hydraulic conductivity of the medullary bundles and the secondary xylem. The contribution of medullary bundles to the total potential hydraulic conductivity was estimated by the ratio of these conductivities. The contribution of the secondary xylem to the total potential hydraulic conductivity was estimated by the ratio of these conductivities. The contribution of medullary bundles and secondary xylem was modeled for three stages of development using linear regression models.

Results

Medullary bundles are structurally diverse, and other patterns of conducting vascular tissue in the pith are present

Two types of eustele occur in Caryophyllales: (1) typical eustele (without medullary bundles; Figs 1a–c, S3); and (2) polycyclic eustele, with medullary bundles that can be collateral or amphivasal (Figs 1d,e, S3). Medullary bundles, which are considered a type of conducting vascular tissue in the pith (CVTP), arise from procambial leaf/bud and/or thorn traces and establish in the pith during primary growth in addition to vascular bundles that delimit the pith (Figs 2a, 3a,b). Medullary bundles are collateral in most taxa (Fig. 3a) and amphivasal in other species (e.g. *Gallesia integrifolia*; Fig. 1e). Medullary bundles develop a cambium and, therefore, undergo secondary growth, in this case, called 'vascular fascicle' (Fig. 3c,d). Cambial activity is evident by the presence of secondary vascular tissues, including conducting and nonconducting phloem that collapses (Fig. 3c,d). Intact sieve tube elements are observed in medullary bundles of developed stems (Fig. 3c). The number of medullary bundles varied from 2 to > 30, displaying various arrangements (e.g. opposite poles, parallel, rings, scattered) as seen in cross-section (Figs 1d, 2a, 3a, S4).

Besides medullary bundles (CVTP – TYPE 1), two other patterns of CVTP are defined (Fig. 2; Table 1): TYPE 2 is represented by vascular bundles of the typical eustele, which become seemingly immersed in the pith. This is because the first cambium originates independently from the primary vasculature and is, therefore, called extra-fascicular cambium (Figs 1f, 2b). This pattern is observed in some Amaranthaceae s.str., Chenopodiaceae, and Nyctaginaceae (Tables S1, S2). TYPE 3 is the presentation of strands of phloem or complete vascular bundles that develop from cells in the perimedullary region (Fig. 2c). These conducting vascular units develop asynchronously after secondary growth has begun. This type is observed in some Caryophyllaceae and Polygonaceae (Table S1; also see Maheshwari & Singh, 1942; Carlquist, 2001).

Medullary bundles appeared independently multiple times

Comparisons of transformation parameters indicated speciational kappa (κ) as the best-fit model for the evolution of medullary bundles (AIC = 346.50), where $\kappa < 1$ (Table S4) indicates that

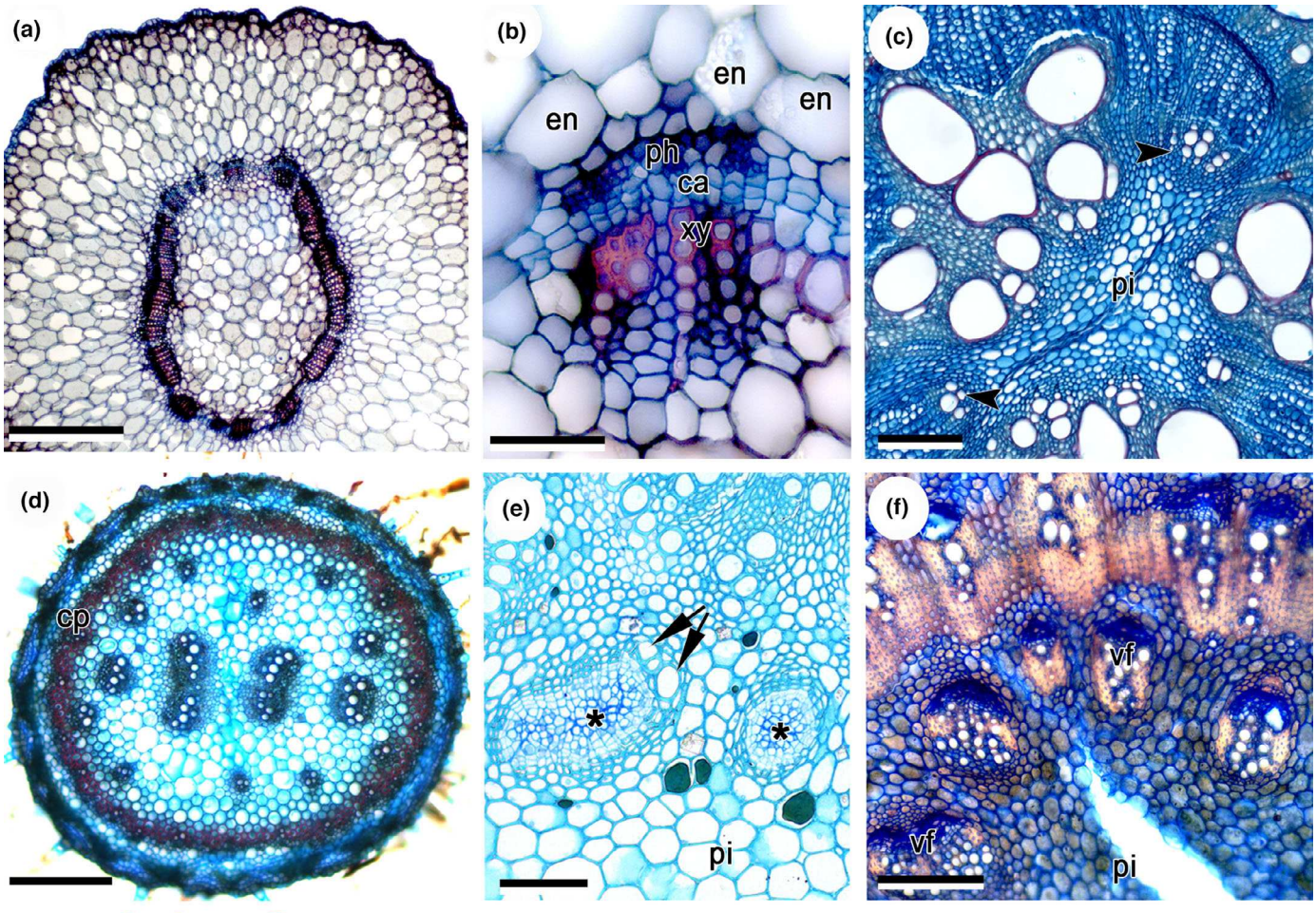

Fig. 1 Anatomical diversity of eustele types in Caryophyllales. (a–c) Typical eustele. (a) *Portulaca halimoides*, Portulacaceae – general view of typical eustele (without medullary bundles). (b) *Sesuvium sesuvioides*, Aizoaceae – detail of cambium in early secondary growth. (c) *Agdestis clematidea*, Agdestidaceae – pith without medullary bundles. Arrowheads indicate the primary xylem. (d–f) Polycyclic eustele. (d) *Mirabilis albida*, Nyctaginaceae – stem in early secondary growth showing medullary bundles scattered in the pith. The cambium is established from the vascular bundles formed by the continuous procambium (cp). (e) *Gallesia integrifolia*, Petiveriaceae – amphivasal medullary bundles; note phloem (asterisks) surrounded by the cambium producing vessels (arrow) outwards. (f) *Charpentiera obovata*, Amaranthaceae – vascular bundles with secondary growth (vascular fascicle), originated from the typical eustele. The extra-fascicular cambium originates in the transition to secondary growth and determines the position of the vascular fascicles as independent units 'isolated' in the pith. ca, cambium; cp, continuous procambium; en, endodermis; mb, medullary bundle; ph, phloem; pi, pith; vf, vascular fascicle; xy, xylem. Bars: (a, c, d) 500 μm; (b) 50 μm; (e, f) 100 μm. Stained with toluidine blue (a, e). Stained with safrablau (b, d, f).

short branches had a higher contribution for the evolution of this character compared with long branches. Plotting changes through time indicates an accelerated early evolution before the diversification of the crown clade of Caryophyllales (Fig. 4). However, the evolution of medullary bundles occurred mainly in the last 10 Myr, such as in Cactoideae (Cactaceae) and Nepenthaceae (Fig. 4). The ancestor of Caryophyllales was inferred with typical eustele (without medullary bundles; Fig. 4; best-fit model ARD; AIC = 373.61; Table S4). In the evolutionary history of Caryophyllales history, medullary bundles arose 36.7 ± 5.2 times on average (gains) in both core and noncore families, with an average of 65.1 ± 11.8 reversals to a typical eustele (losses). The bulk of gains of medullary bundles occurred in Amaranthaceae s.str., Cactaceae, Nepenthaceae, and Nyctaginaceae, with minor events in Chenopodiaceae, Droseraceae, Petiveriaceae, and Phytolaccaceae (Fig. 4). Medullary bundles are conserved in Nyctaginaceae, while the evolutionary history of this character is more complex in Amaranthaceae s.str. and Cactaceae. In these lineages, losses were highly homoplastic even in closely related taxa within these clades. Pagel's (1994) test of correlated evolution infers that medullary bundles and successive cambia are slightly correlated (Pagel's test; $P = 0.004$; phylogenetic signal: $\lambda = 1.00$ and $\lambda = 0.95$, respectively; Fig. 5; Table S5).

Diversification rate heterogeneity is not explained by transitions to polycyclic eustele (medullary bundles), but species with this trait have higher diversification rates

We found heterogeneity in the diversification rate across the phylogeny of Caryophyllales. We detected 27 and 30 diversification

New Phytologist

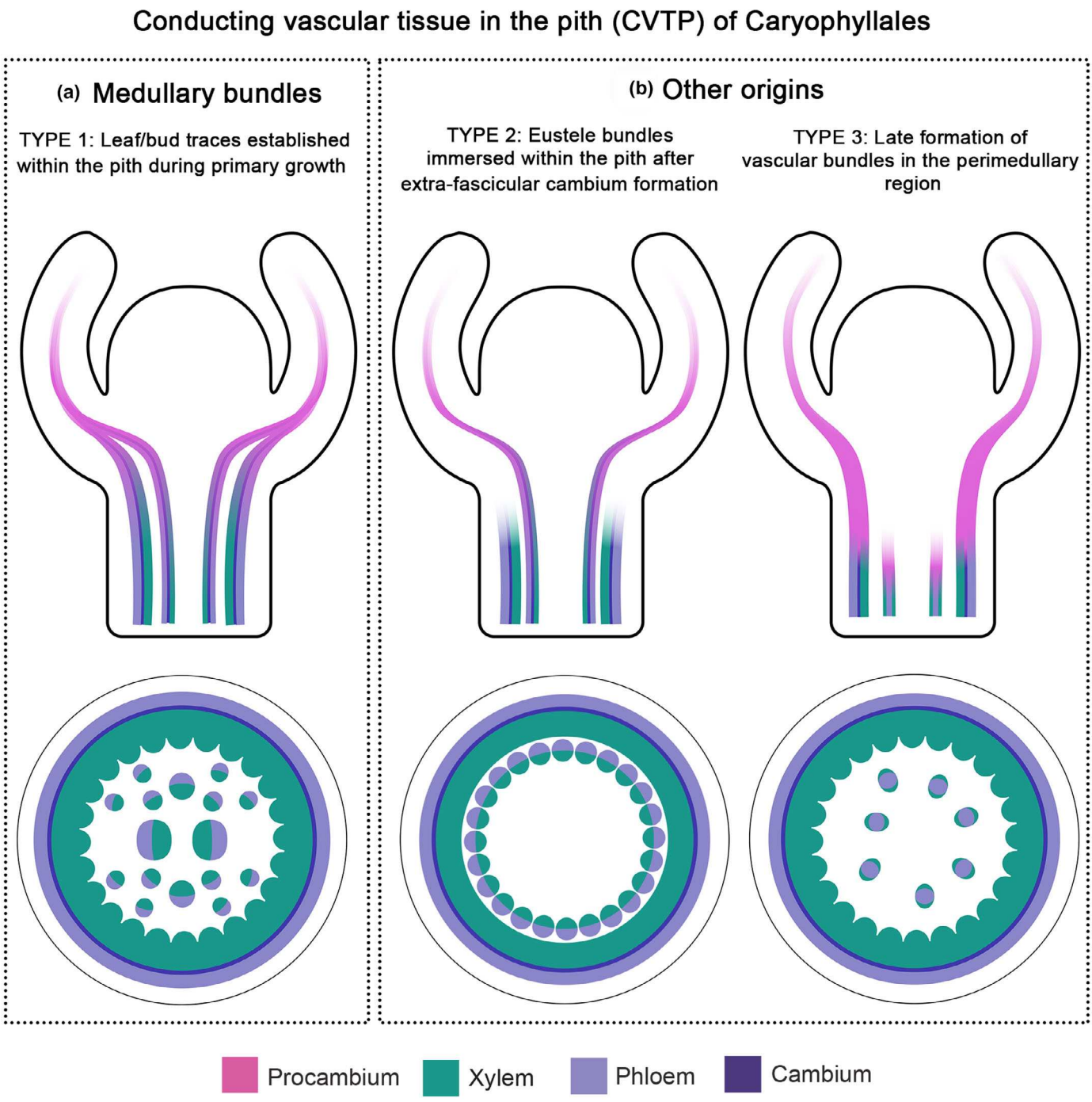

Fig. 2 Developmental diversity of conducting vascular tissue in the pith (CVTP) across Caryophyllales. Longitudinal drawings (upper part of the figure) illustrate the shoot apical meristem; cross views in the lower part of the figure represent stems during the transition from primary to secondary growth (apical internodes). The change from pink to purple indicates the transition from the procambium to the cambium, accompanied by xylem and phloem. (a) Medullary bundles (TYPE 1) arise from vascular traces of leaves, branches, and/or thorns that deviate toward the pith (inner vascular bundles). Medullary bundles emerge early in development, near the shoot apex, and constitute the stele. Note the stele bundles delimiting the pith (outer vascular bundles). (b) Two other cases of CVTP (not considered typical medullary bundles). TYPE 2, vascular bundles of the stele (inner bundles) assume a medullary position due to the formation of a cambium outside the primary vasculature, that is extra-fascicular cambium (outer vascular tissue). See also Wilson (1924) and Balfour (1965). TYPE 3, phloem strands or complete vascular bundles arise in later developmental stages in the perimedullary region (inner bundles). See also Maheshwari (1929), Joshi (1936), and Maheshwari and Singh (1942).

rate shifts, with MEDUSA and BAMM, respectively, from which 16 shifts are shared by both methods (Figs 6a, S5). These shifts appeared in *Nepenthes*, *Tamarix*, *Rumex*, and *Atriplex* and in distinct lineages within Aizoaceae and Nyctaginaceae (Fig. S5). We evaluated the contribution of medullary bundles to the diversification rate. Using AIC model selection, for the two series of

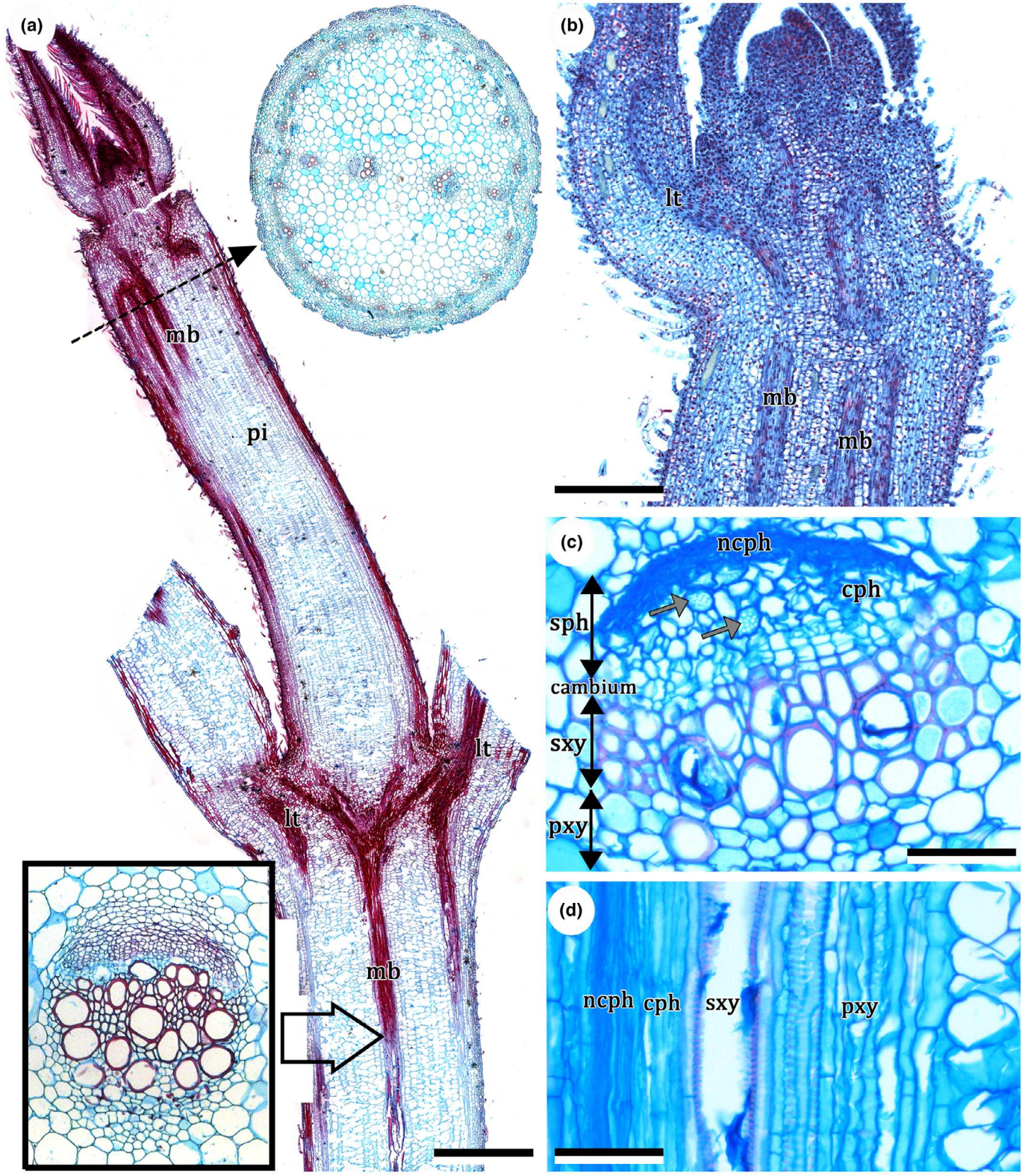

Fig. 3 Origin and anatomy of medullary bundles. (a) *Alternanthera brasiliana*, Amaranthaceae – longitudinal section and cross-section details of medullary bundles originating from leaf traces, which diverge toward the pith. Upper right inset indicates a cross section showing four medullary bundles organized in parallel, and the lower left inset shows a collateral medullary bundle. Note anastomoses between bundles in the node. (b) *Bougainvillea stipitata*, Nyctaginaceae – shoot apex with leaf traces diverging toward the pith and constituting medullary bundles. (c, d) *Pisonia aculeata*, Nyctaginaceae – vascular fascicle (medullary bundle with secondary growth); note the conducting and nonconducting phloem, with collapsed cells. Arrow (gray), sieve tube element; cph, conducting phloem; lt, leaf trace; mb, medullary bundle; ncph, nonconducting phloem; pi, pith; pxy, primary xylem; sph, secondary phloem; sxy, secondary xylem. Bars: (a) 500 μm; (b) 50 μm; (c, d) 100 μm. Stained with safranin and astra blue (a–d).

Table 1 Phylogenetic distribution of conducting vascular tissue in the pith (CVTP) across Caryophyllales.

Family	Sampling (genera/species)	Medullary bundles	Other CVTP[1]	Bundle type
Achatocarpaceae	2/2	0	–	–
Agdestidaceae	1/1	0	–	–
Aizoaceae	32/49	0	–	–
Amaranthaceae s.str.	23/59	1	TYPE 2	Collateral[1]
Anacampserotaceae	3/7	0	–	–
Ancistrocladaceae	1/1	0	–	–
Asteropeiaceae	1/1	0	–	–
Barbeuiaceae	1/1	0	–	–
Basellaceae	2/3	0	–	–
Cactaceae	96/313	1	–	Amphivasal[2], Collateral
Caryophyllaceae	16/34	0	TYPE 3	–
Chenopodiaceae	33/70	1	TYPE 2	Collateral
Didiereaceae	5/14	0	–	–
Dioncophyllaceae	3/3	0	–	–
Droseraceae	3/33	1	–	Collateral
Drosophyllaceae	1/1	0	–	–
Frankeniaceae	1/3	0	–	–
Gisekiaceae	1/1	0	–	–
Halophytaceae	1/1	0	–	–
Kewaceae	1/2	0	–	–
Limeaceae	1/3	0	–	–
Lophiocarpaceae	2/3	0	–	–
Macarthuriaceae	1/2	0	–	–
Microteaceae	1/1	0	–	–
Molluginaceae	5/9	0	–	–
Montiaceae	4/4	0	–	–
Nepenthaceae	1/38	1	–	Amphivasal, Collateral
Nyctaginaceae	24/83	1	TYPE 2	Collateral
Petiveriaceae	9/10	0	–	–
Physenaceae	1/1	0	–	–
Phytolaccaceae	3/10	1	–	Collateral, Amphivasal[3]
Plumbaginaceae	5/20	1	–	Collateral
Polygonaceae	16/48	1	TYPE 3	Amphivasal[4], Collateral
Portulacaceae	1/8	0	–	–
Rhabdodendraceae	1/2	0	–	–
Sarcobataceae	1/1	0	–	–
Simmondsiaceae	1/1	0	–	–
Stegnospermataceae	1/3	0	–	–
Talinaceae	1/6	0	–	–
Tamaricaceae	2/6	0	–	–

Sampling (genera/species) indicates the total number of genera and species investigated in this study. Medullary bundles: 0, absence; 1, presence. See Supporting Information Table S1 for information on the species level. Family classification follows Hernández-Ledesma *et al*. (2015).

[1]Collateral bundles = bundles having xylem and phloem on opposite sides.

[2]Amphivasal bundles = bundles having xylem surrounding the phloem tissue from all sides.

[3]Bundles tend to assume this form after secondary growth (Kirchoff & Fahn, 1984).

[4]Bundles tend to assume this form after continued secondary growth (Maheshwari & Singh, 1942).

analyses the preferred model was HiSSE (Fig. 6b; Table S6), in which an unobserved trait, not the medullary bundles, better explains the diversification rate dynamics. Nevertheless, the diversification rate of the species that have medullary bundles is significantly higher than that of those without them ($P < 2.2e\text{-}16$; Fig. 6c), indicating that the presence of medullary bundles might be important for the diversification of the species in Caryophyllales along with other factors.

Medullary bundles are functionally conductive throughout the plant's lifespan and have a major contribution to hydraulic conductivity in herbaceous plants

We characterized the conduction activity of medullary bundles (Experiment 1) and the potential conductivity of the xylem of medullary bundles in comparison with the secondary xylem in the vascular cylinder in plants with distinct growth habits and growing in different environments (Fig. 7). Experiment 1 confirms that medullary bundles are actively conducting water even in developed stems of *Mirabilis jalapa* (Fig. 8a) and *Bougainvillea spectabilis* (Fig. S1). Vessels in medullary bundles and the secondary xylem are stained with safranin in *M. jalapa* at an average maximum distance of 16.3 ± 3.0 and 14 ± 2 cm, respectively, while in *B. spectabilis* their average maximum distance is of 12 ± 3.6 and 18.3 ± 6 cm, respectively (Fig. S1; Table S7). In addition, medullary bundles connect through the main stem and lateral branches (Fig. S2). Next, we demonstrated the contribution of medullary bundles to total potential conductivity of the stems (Experiment 2) by estimating their conductivity in three different developmental stages (Fig. 8b–d). At the beginning of development, medullary bundles contribute on average 96 ± 2% to the total potential conductivity of the stems near the apex in all species. As the stem develops, the contribution of medullary bundles to the total potential conductivity decreases in more developed stems (*P. glabrata*) or near the base of the plants (*A. incarnata* and *M. jalapa*), remaining on average 58 ± 30% in herbaceous species (Fig. 7b, c) and 17 ± 22% in *P. glabrata* (Fig. 8d), shrubby liana. On the contrary, vessels in the secondary xylem increase their contribution to the total potential conductivity throughout stem development in all species (Fig. 8a–c). In herbaceous species, the secondary xylem development near the stem base contributes to total potential conductivity on average with 42 ± 30%, and in lianescent species 83 ± 22% (Fig. 8a–d).

Discussion

Conducting vascular tissue in the pith develops in different ways

Our findings demonstrate that typical medullary bundles are not the only type of conducting vascular tissues in the pith (CVTP) in Caryophyllales. Considering their developmental origin, medullary bundles (CVTP – TYPE 1) have been classified into

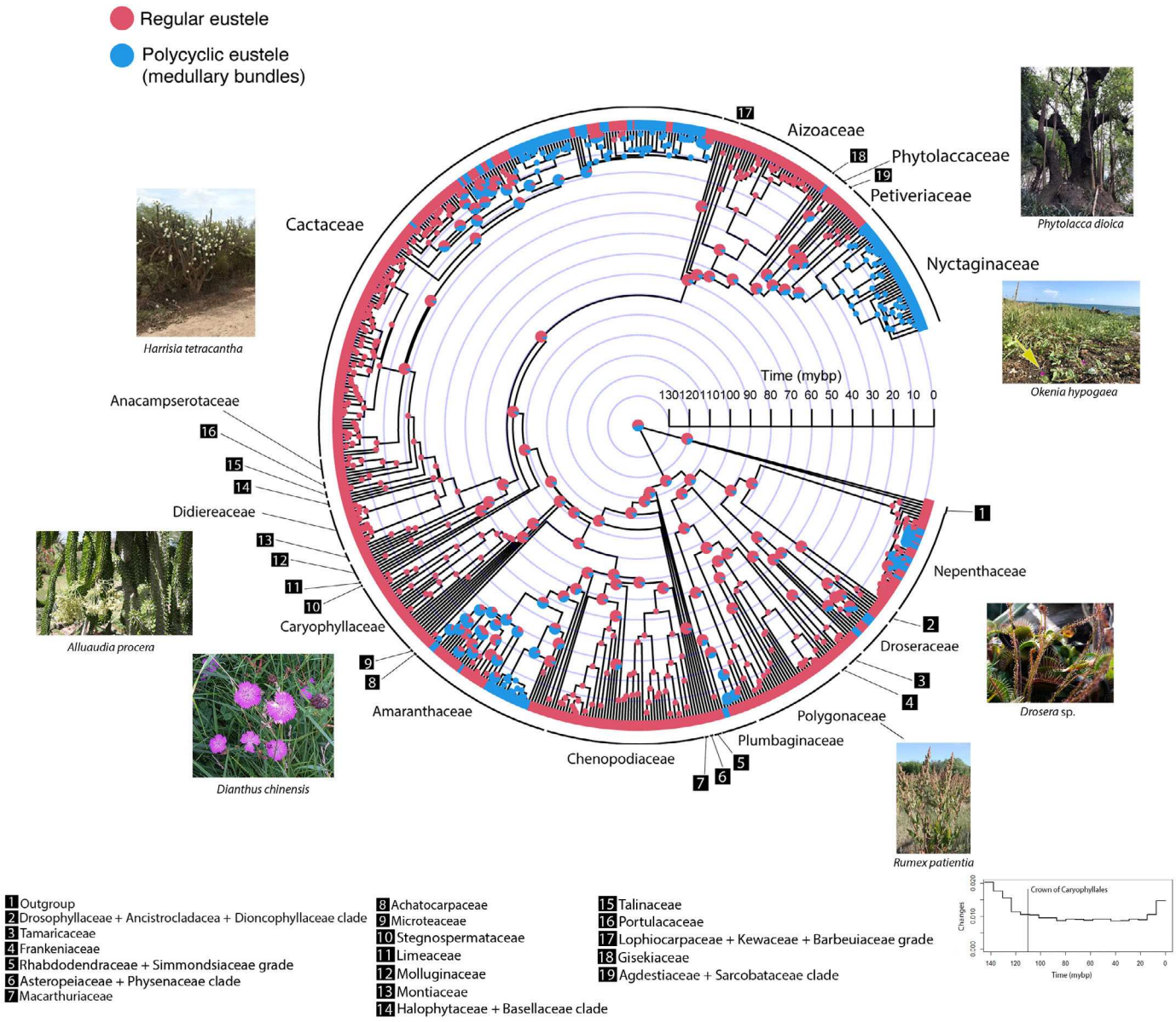

Fig. 4 Ancestral state reconstructions of eustele types from 1000 stochastic mapping simulations across the Caryophyllales phylogeny. Only the presence of medullary bundles is included in the analyses; other types of conducting vascular tissue in the pith (type 1 and type 2) are not included. Pie charts of nodes with posterior probabilities (PP) support ≤ 0.95 are three times larger than pie charts of nodes with PP support > 0.95. Photo credit: *Harrisia tetracantha* (courtesy of Michael H. Nee). mybp, millions of years before present. Note plot indicating the number of transitions through time (bottom right). [Correction added on 11 January 2024, after first online publication: data points in the diagram in the centre of the figure have been updated.]

two main categories (De Bary, 1884; Wilson, 1924; Kirchoff & Fahn, 1984): (1) bundles originated from procambial leaf/bud traces; and (2) bundles that are not associated with procambial leaf/bud traces (i.e. 'cauline bundles'). Nevertheless, 'cauline bundles' originate also from divisions of sympodial bundles in the nodal region (Wilson, 1924), which may indicate their relationship to leaf primordia (and procambial origin). In terms of development, medullary bundles in Cactaceae have been described as 'cauline bundles' (Gibson, 1976), as well as arising close to the shoot apex (Boke, 1941, 1951), from a rib meristem (Macdougal, 1926; Boke, 1941) or from the procambium (Boke, 1980). In addition, they have been observed in adult specimens but not in the seedlings of some cacti (Loza-Cornejo & Terrazas, 2011). These contrasting observations may result from the diverse (yet typical) shoot apical meristem of cacti (Mauseth, 2006). While these observations suggest a procambial origin for medullary bundles (i.e. CVTP – TYPE 1) in this lineage, further developmental studies would expand upon this concept. The different types of CVTP are not comprehensively distinguished in the literature, and the term medullary bundles is used interchangeably to describe these disparate processes (Wilson, 1924), including cases of 'bicollateral bundles' (Bogle, 1969; Carlquist, 1999). Here, the term 'medullary bundles' is used for cases of vascular bundles forming polycyclic eusteles which usually originate from procambial

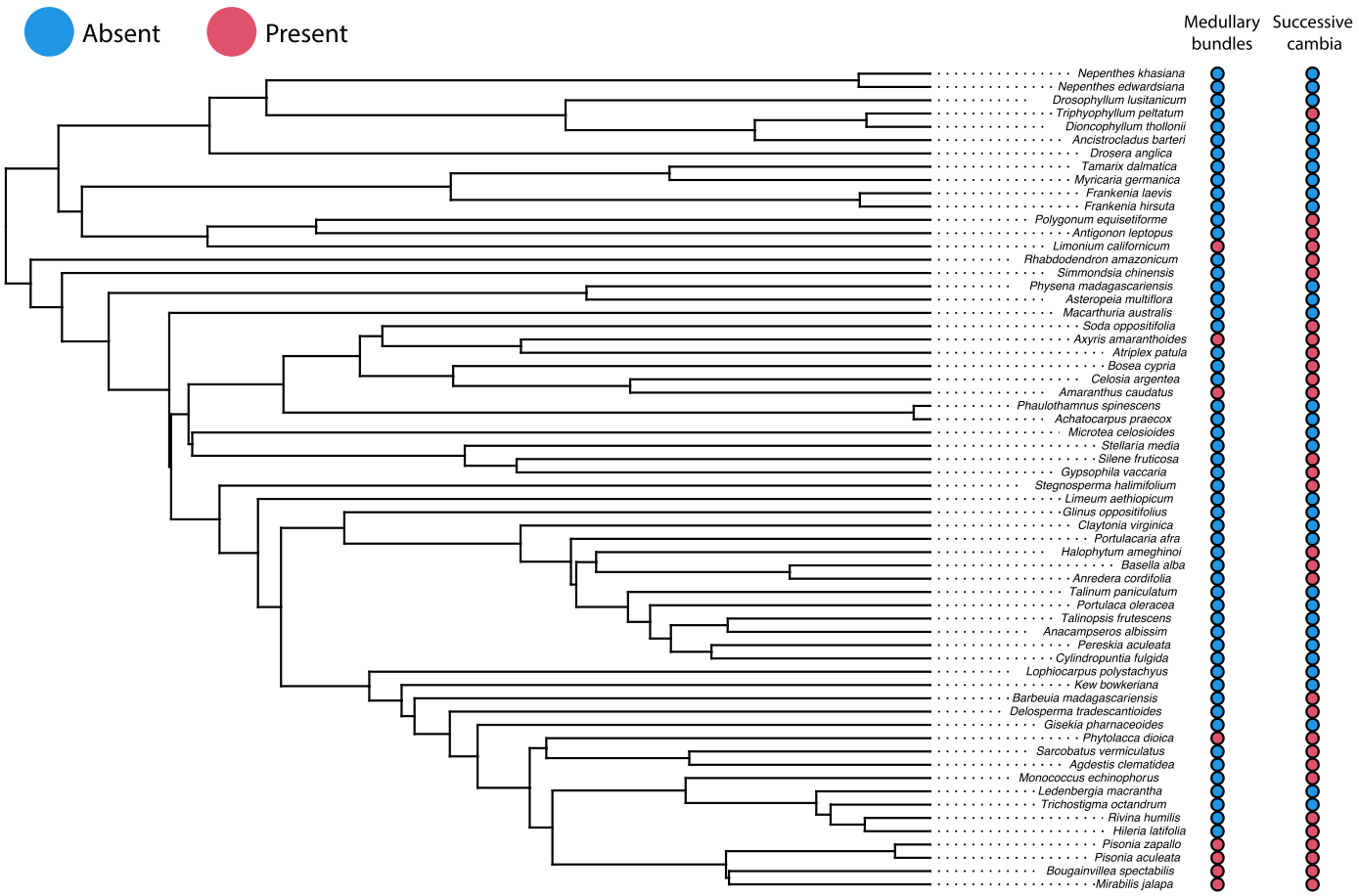

Fig. 5 Pagel's (1994) analysis for detecting 'correlated' evolution of medullary bundles and successive cambia in Caryophyllales. Medullary bundles and successive cambia are correlated (Pagel's test; $P < 0.05$), suggesting that traits are constrained to evolve together.

traces, emerging during primary growth, and with stable establishment within the pith at early developmental stages, near the shoot apex (i.e. CVTP – TYPE 1).

An accurate distribution of CVTP – TYPE 2 and 3 across Caryophyllales would require further developmental studies to separate these similar anatomies in some lineages. For instance, the occurrence of CVTP – TYPE 2 in species of Nyctaginaceae was recently revealed through ontogenetic studies (Cunha Neto *et al.*, 2022). This pattern is also present in Chenopodiaceae (Wilson, 1924) and seems to occur in some Amaranthaceae (ILCN pers. observ.), including *Celosia argentea* which is described as having 'the first cambium within the procambium-derived zone, which is distinct above the primary bundles' (Myśkow *et al.*, 2019, p. 1464). As for CVTP – TYPE 3, vascular bundles derive from procambial remnants in Polygonaceae (Maheshwari, 1929), but might result from a *de novo* vascular meristem in Caryophyllaceae (Pfeiffer, 1926; Carlquist, 2001). The identification of multiple categories of CVTP indicates that typical medullary bundles (CVTP – 1) are likely present in fewer lineages than previously believed, while other developmental processes have contributed to the evolution of CVTP in Caryophyllales – and other seed plants (e.g. atactostele and ectopic cambia; Philipson & Balfour, 1963; Tomescu, 2021). Notably, different forms of CVTP are present in fossil plants (e.g. Medullosales, fossil Cycadales, and Corystopermales; Artabe & Brea, 2003; Bodnar & Coturel, 2012), indicating that plants have used these vascular architectures for a long time.

Medullary bundles: another remarkable case of convergent evolution across Caryophyllales

At a minimum, there have been 36 independent origins of medullary bundles within Caryophyllales. When examined individually, families with medullary bundles show distinct evolutionary histories which include contrasting scenarios: medullary bundles appear only once in Nyctaginaceae (also see Cunha Neto *et al.*, 2020a) and evolved multiple times within Droseraceae and Nepenthaceae; multiple transitions from typical to polycyclic eustele occur at either the species (e.g. Nepenthaceae) or genus level (e.g. Amaranthaceae); medullary bundles evolved in both species-rich (e.g. Amaranthaceae and Cactaceae) and species-poor (e.g. Droseraceae) families (Table S1). Stochastic character mapping confirms the evolution of medullary bundles in the ancestral node of the subfamily Cactoideae (Cactaceae), with several losses (e.g. tribes Cacteae, Echinocereeae, and Notocacteae). Previous studies predicted this scenario and suggested that the restricted distribution of medullary bundles in Cactoideae is a useful characteristic for the systematics of the family (Mauseth, 1993;

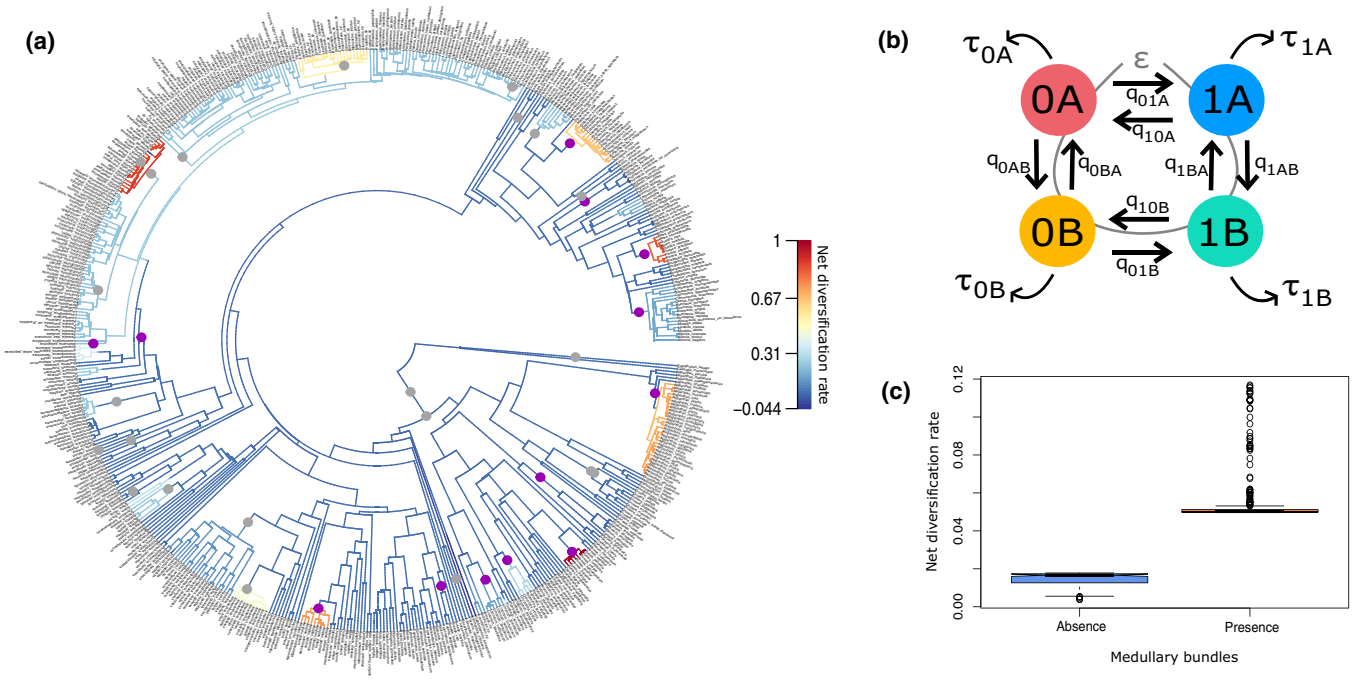

Fig. 6 Diversification dynamics. (a) Net diversification rate across Caryophyllales. Purple circles indicate shifts in diversification rates shared in both BAMM and MEDUSA analyses; gray circles correspond to shifts detected only by BAMM. The color scale indicates net diversification rates. (b) Trait-dependent diversification analysis with HiSSE on the presence of medullary bundles (0 and 1) and a hidden character (A, B). Preferred model with turnover (τ) rates for each state, one rate for extinction fraction (ε), and eight transition rates between states (*q*). (c) Model averaging of the three models with the highest AIC values (Supporting Information Table S6) indicating that lineages with medullary bundles have a significant ($P < 2.2e\text{-}16$) higher net diversification rate.

Terrazas & Arias, 2002; Terrazas Salgado & Mauseth, 2002; Franco-Estrada *et al.*, 2021).

Previously, medullary bundles were ancestrally reconstructed for the phytolaccoid clade (including the families Agdestidaceae, Nyctaginaceae, Phytolaccaceae, Petiveriaceae, and Sarcobataceae; Cunha Neto *et al.*, 2020a). In the present study, however, medullary bundles were not present in the node of this clade, with independent gains in *Phytolacca dioica* (Phytolaccaceae), *Gallesia integrifolia* (Petiveriaceae) and once in Nyctaginaceae. Although present in all representatives of *Amaranthus* and related genera, the evolution of medullary bundles in Amaranthaceae s.str. is complex since there are multiple gains and losses (e.g. Gomphrenoideae and Achyranthoids clades). Medullary bundles evolved exclusively through independent origins in the two largest carnivorous families. This represents the lineages with the smaller number of species with this feature. In Droseraceae, medullary bundles are reported for only four species of *Drosera* (DeBuhr, 1977), which are included either in subgenera *Drosera* or *Ergaleium* (classification based on Rivadavia *et al.*, 2003). Similarly, medullary bundles were found independently in eight species of Nepenthaceae (Schwallier *et al.*, 2017), which are nested in sections Montanae, Pyrophytae, or Regiae (classification based on Clarke *et al.*, 2018); these sections are nested in multiple clades correlated to distinct geographic regions, although all included in a larger phylogenetic lineage (i.e. Clade 2, classification based on Murphy *et al.*, 2020). Taken together, these observations demonstrate that the evolution of medullary bundles is highly homoplastic in Caryophyllales, an evolutionary pattern that is also reported to other morphological adaptations in the order (e.g. pigmentation: Brockington *et al.*, 2011, 2015; Timoneda *et al.*, 2019; flower traits: Ronse De Craene, 2013; Ronse de Craene, 2021; fruit types: Sukhorukov *et al.*, 2015, 2021, 2023; and successive cambia: Schwallier *et al.*, 2017).

Here, it is demonstrated that medullary bundles and successive cambia evolved in a correlated fashion in Caryophyllales (Pagel's 1994 test of correlated evolution). Although this conclusion provides evidence indicating that these two traits may be part of the same adaptive network, such correlation could be due to other factors, and experimental research is needed to support these findings (Maddison & FitzJohn, 2015). The enormous developmental plasticity and evolutionary lability in disparate morphological features across the Caryophyllales including vascular development provide substantial opportunities for functional and comparative molecular studies across the order.

Acquisition of medullary bundles does not explain shifts in diversification rates in Caryophyllales

The hypothesis that medullary bundles led to increased diversification is not supported in this study. Previous results indicated an association between medullary bundles and increased diversification rates in the phytolaccoid clade (Cunha Neto *et al.*, 2022) but may have been influenced by the prevalence of medullary bundles in Nyctaginaceae, where only four species have a typical

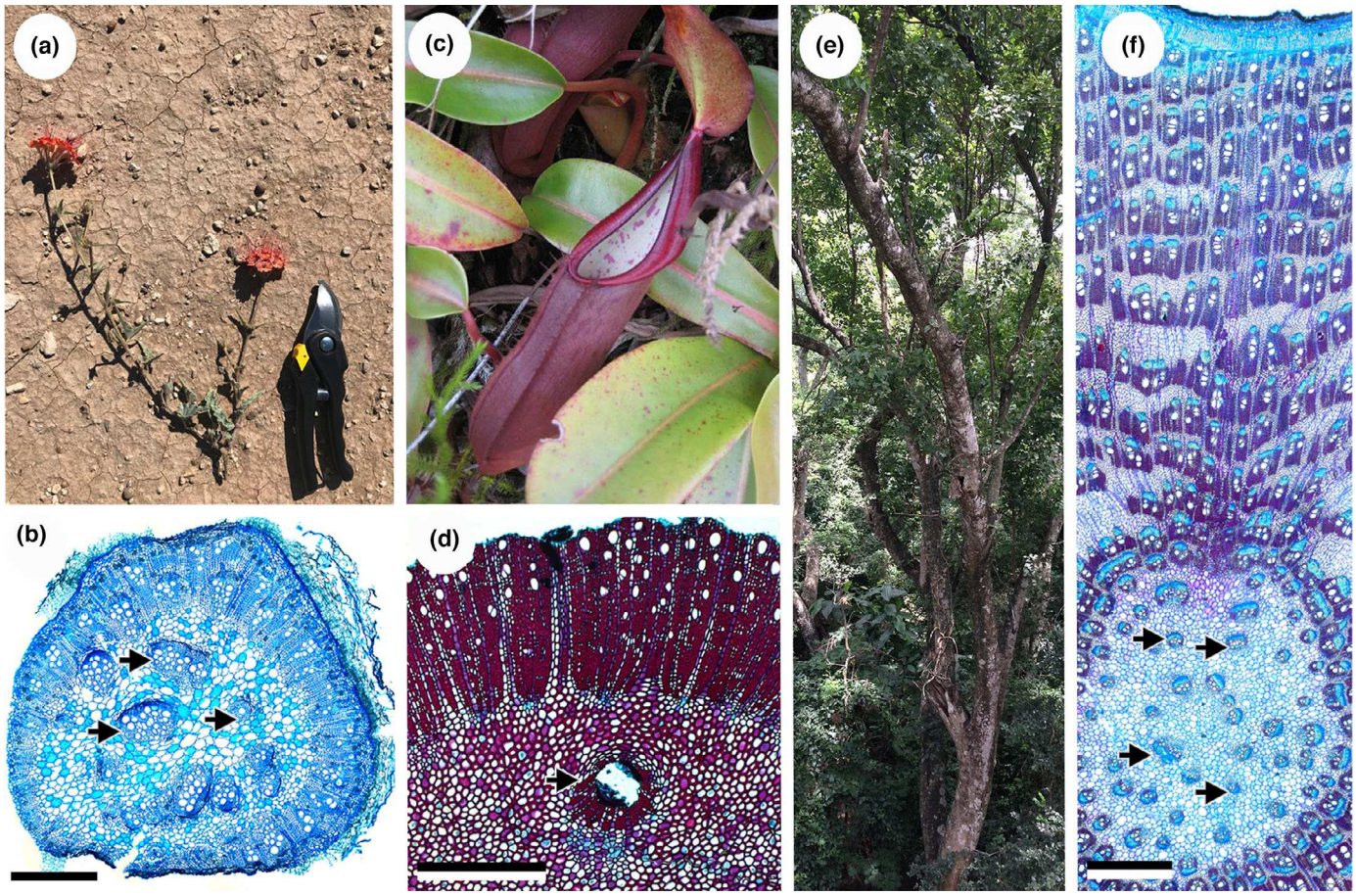

Fig. 7 External morphology and anatomical aspects of herbaceous and woody plants with medullary bundles. (a, b) *Nyctaginia capitata*, Nyctaginaceae – herbaceous plant with seven to eight medullary bundles (arrows) in unordered arrangement. (c, d) *Nepenthes sanguinea*, Nepenthaceae – herbaceous plant showing detail of a single medullary bundle (arrow). (e, f) *Bougainvillea modesta*, Nyctaginaceae – tree with numerous medullary bundles in unordered arrangement. Photo credit: (c) Wikimedia (CC BY-SA 3.0): David Tan (www.petpitcher.com); (d) courtesy of Rachel Schwallier. Bars: (b, d, f) 500 µm. Stained with safranin and astra blue (b, d, f).

eustele. In other words, this could be interpreted as a case of pseudoreplication within a lineage (Maddison & FitzJohn, 2015). Twenty-six shifts in diversification rates across the phylogeny of Caryophyllales have been found, similar to the results obtained by Smith *et al.* (2018; also using MEDUSA). Smith *et al.* (2018) reported that four diversification shifts were concurrent with whole genome duplications (WGD) and argued that they often occur along with shifts in either diversification rate, climate adaptation, or morphological evolutionary rate. Some WGD events and diversification rate shifts probably occurred synchronously, for example on the branch leading to the tribe Nyctagineae (Nyctaginaceae), *Amaranthus*, Droseraceae, and Nepenthaceae. This may explain the findings, in that while diversification rates were significantly higher in species with medullary bundles, the joint effect of multiple factors likely influenced species diversification in this order. For example, other remarkable traits of Caryophyllales (e.g. betalains) were demonstrated to have evolved in correlation with lineage-specific gene duplications, associated with key changes in metabolic pathways through neofunctionalization (Brockington *et al.*, 2015; Yang *et al.*, 2015). The repeated evolution of extraordinary morphological and physiological traits, including vascular adaptations such as CVTP and vascular variants, may hence be associated with novel gene networks, duplicated gene lineages, and polyploidy throughout the evolutionary history of Caryophyllales (Yang *et al.*, 2018).

The number and arrangement of medullary bundles in transection are diverse and have taxonomic value

Both collateral and amphivasal bundles are observed in Caryophyllales (Table 1). These are conserved within lineages, with a few exceptions where both types may occur (e.g. Cactaceae) and for which systematic implications may result (Terrazas & Loza-Cornejo, 2002). The number of medullary bundles is highly variable ranging from two to bundles in excess of one hundred in some columnar cacti (Gibson & Nobel, 1986). Regardless of their type and number, medullary bundles can be irregularly distributed (nonordered, scattered) or distributed equidistantly (ordered; Terrazas & Loza-Cornejo, 2002; Cunha Neto *et al.*, 2020a). The disparate number and arrangement of medullary bundles have systematic significance in Nyctaginaceae (e.g. distinction between different species of *Pisonia*: Cunha Neto *et al.*, 2020a).

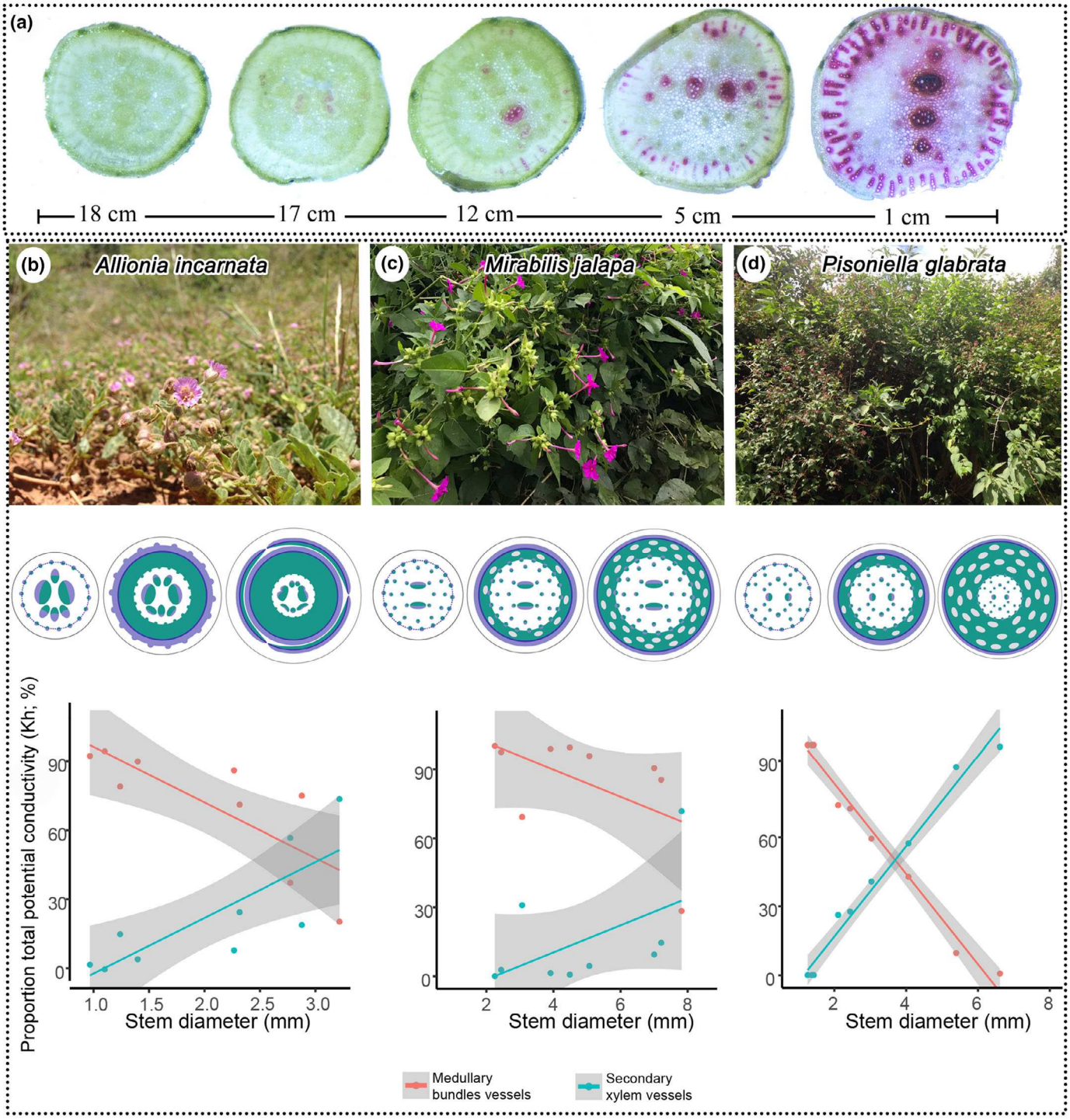

Fig. 8 Form–function relations of medullary bundles in Nyctaginaceae (Caryophyllales). (a) A set of cross sections (from top to bottom) from a branch of *Mirabilis jalapa* shows the secondary xylem and medullary bundles stained at different heights (from top-18 cm to bottom-1 cm of the stem). Because vessels in medullary bundles are stained by safranin, it indicates that they are functionally conducting water. See also Supporting Information Fig. S1 for images of the same experiment with *Bougainvillea spectabilis*. (b–d) Proportion of total potential conductivity in species with distinct habits: *Allionia incarnata* – herb (b), *Mirabilis jalapa* – perennial herb (c), and *Pisoniella glabrata* – liana (d). Top section of each panel shows plants in the field, the middle section shows drawings of stem cross sections in three developmental stages (primary growth, early secondary growth, and mature stem), and the bottom section shows plots indicating the contribution of medullary bundles to total potential conductivity; note that hydraulic contribution of medullary bundles diminishes in relation to the secondary xylem in all species but remain near 50% in herbaceous plants.

Secondary growth in medullary bundles is common (Mauseth, 1993; Cunha Neto *et al.*, 2020a) and is associated with the conversion of collateral bundles into amphivasal bundles (e.g. *Phytolacca dioica*: Kirchoff & Fahn, 1984). The occurrence of fibers within the medullary bundles is also variable across species of Cactaceae (Mauseth, 1993; Terrazas & Loza-Cornejo, 2002).

What is the functional significance of medullary bundles?

One of the functional roles of medullary bundles is their ability to increase water and sugar conduction and accumulation (Haberlandt, 1914; Gibson & Nobel, 1986; Terrazas Salgado & Mauseth, 2002), and our anatomical and hydraulic data support these roles. The hydraulic data demonstrate that medullary bundles are not only functionally active in young stems but also largely contribute to total conductivity throughout stem development, especially in herbaceous species. In contrast, secondary vascular tissues provide most of the hydraulic conductivity in larger woody plants, and the contribution of medullary bundles decreases significantly. Medullary bundles are also confirmed to undergo secondary growth, which adds extra conducting elements and eventually rays to their structure (Mauseth, 1993; Cunha Neto *et al.*, 2020a), and the accumulation of starch grains in pith cells surrounding them provides additional evidence of their functional role (Mauseth, 1993; Soffiatti & Angyalossy, 2007; Aguilar *et al.*, 2009; Cunha Neto *et al.*, 2020a). Medullary bundles also anastomose among themselves and with the main vascular system (Boke, 1951; DeBuhr, 1977; Mauseth, 1993), or with cortical bundles where they occur (e.g. Cactaceae). The ability to produce supplemental vascular tissue in three-dimensional arrangements in the vascular system (e.g. medullary bundles) likely represents a functional advantage for plants growing in conditions of physiological drought, similar to vascular networks in the secondary vascular system (e.g. successive cambia or interxylary phloem; Hearn, 2009, 2019; Robert *et al.*, 2014; Cirillo *et al.*, 2017; Grigore & Toma, 2017; Bouda *et al.*, 2022).

The vascular network organization created along with medullary bundles leads to greater stem vascularization in the shoots (Mauseth, 2004; Hearn, 2009), which may be significant in reducing the risk of hydraulic failure in plants (Bouda *et al.*, 2022; Lens *et al.*, 2022). That is particularly relevant in xerophytic plants, for example, columnar cacti, in which the major presence of medullary bundles has been hypothesized to have increased hydraulic functions, which facilitated the evolution of their large stems (Gibson & Nobel, 1986; Mauseth, 1993; Terrazas Salgado & Mauseth, 2002). The correlation between drought and the presence of medullary bundles is not universal, since several xerophytic families lack medullary bundles (e.g. Aizoaceae, Anacampserotaceae, Frankeniaceae, and Didiereaceae). In these cases, other adaptations could play a more significant role in response to drought stress in plants growing in xeric environments. For instance, successive cambia are present in many Aizoaceae (Carlquist, 2007) and in some Frankeniaceae (Barghoorn, 1941), demonstrating the contribution of these vascular variants to plant growth and survival (Carlquist, 2001; Grigore & Toma, 2017).

Conclusion

Considered a 'most promising field for anatomo-physiological research' since the early 19th century (Haberlandt, 1914, pp. 381–382), the diversity and evolution of medullary bundles is still unclear in most lineages of angiosperms. Specifically, there has been a lack of research exploring the relationship between this remarkable architecture and other developmental processes that generate disparate CVTP and the functional and evolutionary consequences of that diversity. Conducting vascular tissue in the pith has been shown to develop in three ways in Caryophyllales. Medullary bundles, the most remarkable of all, evolved in a convergent fashion, but their acquisition does not explain shifts in diversification rates in Caryophyllales. Medullary bundles are functionally active and play an important role in hydraulic conductivity, most importantly in herbaceous plants. This comprehensive comparative analysis of the form and function of medullary bundles in Caryophyllales exposes significant evolutionary patterns that may guide future hypotheses at testing plants with medullary bundles on various ecological and evolutionary scales. Researchers in evolutionary developmental biology will find medullary bundles and their propensity to evolve in Caryophyllales an exciting avenue of pursuit.

Acknowledgements

We are indebted to numerous researchers for assistance during field collection. We thank Mariana Victório and Maya V. Nilova for helping with histological analysis, Marcelo R. Pace for providing stem samples, João Fernando M. Silva for helping with R scripts for ASR, Cora Oberst for proofreading the manuscript, and Rubens K. Ito for support with drawings. We are thankful for the herbaria and wood collections for providing samples for anatomical studies. We appreciate the constructive and insightful comments of three reviewers (two anonymous and Prof. Mihai Tomescu), and the handling editor, Prof. Jennifer McElwain. This work was supported by Fundação de Amparo à Pesquisa do Estado de São Paulo (FAPESP – grants 2017/17107-3 to ILCN & 2020/14338-7 to VA) and the Coordenação de Aperfeiçoamento de Pessoal de Nível Superior (CAPES – Finance Code 001 to CSG). The study design of APS and MK is in accordance with the scientific programs 12-2-21 and AAAA-A16-116021660106-0 of the Department of Higher Plants and Department of Plant Physiology (Lomonosov Moscow State University) as well as the program 'Priority-2030' of Tomsk State University. Many computations were performed using the computer clusters and data storage resources of the HPCC of UCR, which were funded by grants from National Science Foundation (USA) (MRI-2215705 and MRI-1429826) and National Institutes of Health (USA) (1S10OD016290-01A1).

Competing interests

None declared.

Author contributions

ILCN designed the research and wrote the initial draft with inputs from all authors; ILCN, CSG, APS, MK, GFAM-d-P and VA collected and interpreted anatomical data; EFSR and RH-G performed phylogenetic analysis and ASR with inputs from ILCN and APS; RH-G conducted diversification analyses with

inputs from ILCN, EFSR and APS; CSG conducted hydraulic experiments, with inputs from ILCN. All authors revised and approved the final version of the manuscript.

ORCID

Veronica Angyalossy https://orcid.org/0000-0002-9823-9946
Israel L. Cunha Neto https://orcid.org/0000-0002-0914-9974
Caian S. Gerolamo https://orcid.org/0000-0003-1819-5371
Rebeca Hernández-Gutiérrez https://orcid.org/0000-0003-2026-0080
Maria Kushunina https://orcid.org/0000-0003-2541-6494
Gladys F. A. Melo-de-Pinna https://orcid.org/0000-0003-4924-8755
Elson Felipe S. Rossetto https://orcid.org/0000-0002-6204-4012
Alexander P. Sukhorukov https://orcid.org/0000-0003-2220-826X

Data availability

All data for reproducibility of this work can be accessed in the Supporting Information. Codes for phylogenetic comparative methods and statistical analyses are found at https://github.com/ilcneto/Medullary_Bundles_in_Caryophyllales.

References

Aguilar MAG, Terrazas T, Arias S. 2009. Anatomía caulinar de tres especies del género *Hylocereus* (Berger) Britton & Rose (Cactaceae) en México. *Revista Fitotecnia Mexicana* **32**: 201–208.

Alfaro ME, Brock CD, Banbury BL, Wainwright PC. 2009. Does evolutionary innovation in pharyngeal jaws lead to rapid lineage diversification in labrid fishes? *BMC Evolutionary Biology* **9**: 1–14.

Arruda E, Melo-De-Pinna GF. 2010. Wide-band tracheids (WBTs) of photosynthetic and non-photosynthetic stems in species of Cactaceae. *Journal of the Torrey Botanical Society* **137**: 16–29.

Artabe AE, Brea M. 2003. A new approach to Corystospermales based on Triassic permineralized stems from Argentina. *Alcheringa* **27**: 209–229.

Balfour E. 1965. Anomalous secondary thickening in Chenopodiaceae, Nyctaginaceae and Amaranthaceae. *Phytomorphology* **15**: 111–122.

Barghoorn ES. 1941. The ontogenetic development and phylogenetic specialization of rays in the xylem of dicotyledons-III. The elimination of rays. *Bulletin of the Torrey Botanical Club* **68**: 317.

Beaulieu JM, O'Meara BC. 2016. Detecting hidden diversification shifts in models of trait-dependent speciation and extinction. *Systematic Biology* **65**: 583–601.

Beck CB, Schmid R, Rothwell GW. 1982. Stelar morphology and the primary vascular system of seed plants. *The Botanical Review* **48**: 691–815.

Blomberg SP, Garland T, Ives AR. 2003. Testing for phylogenetic signal in comparative data: behavioral traits are more labile. *Evolution* **57**: 717–745.

Bodnar J, Coturel EP. 2012. El origen y diversificación del crecimiento cambial atípico en plantas fósiles: procesos del desarrollo involucrados. *Boletin de la Sociedad Argentina de Botanica* **47**: 33–70.

Bogle AL. 1969. The genera of Portulacaceae and Basellaceae in the southeastern United States. *Journal of the Arnold Arboretum* **50**: 566–598.

Boke NH. 1941. Zonation in the shoot apices of *Trichocereus spachianus* and *Opuntia cylindrica*. *American Journal of Botany* **28**: 656–664.

Boke NH. 1951. Histogenesis of the vegetative shoot in *Echinocereus*. *American Journal of Botany* **38**: 23–38.

Boke NH. 1980. Developmental morphology and anatomy in Cactaceae. *Bioscience* **30**: 605–610.

Bollback JP. 2006. SIMMAP: stochastic character mapping of discrete traits on phylogenies. *BMC Bioinformatics* **7**: 88.

Bouckaert R, Vaughan TG, Barido-Sottani J, Duchêne S, Fourment M, Gavryushkina A, Heled J, Jones G, Kühnert D, De Maio N *et al.* 2019. BEAST 2.5: an advanced software platform for Bayesian evolutionary analysis. *PLoS Computational Biology* **15**: e1006650.

Bouda M, Huggett BA, Prats KA, Wason JW, Wilson JP, Brodersen CR. 2022. Hydraulic failure as a primary driver of xylem network evolution in early vascular plants. *Science* **378**: 642–646.

Brockington SF, Alexandre R, Ramdial J, Moore MJ, Crawley S, Dhingra A, Hilu K, Soltis DE, Soltisy PS. 2009. Phylogeny of the Caryophyllales sensu lato: revisiting hypotheses on pollination biology and perianth differentiation in the core Caryophyllales. *International Journal of Plant Sciences* **170**: 627–643.

Brockington SF, Walker RH, Glover BJ, Soltis PS, Soltis DE. 2011. Complex pigment evolution in the Caryophyllales. *New Phytologist* **190**: 854–864.

Brockington SF, Yang Y, Gandia-Herrero F, Covshoff S, Hibberd JM, Sage RF, Wong GKS, Moore MJ, Smith SA. 2015. Lineage-specific gene radiations underlie the evolution of novel betalain pigmentation in Caryophyllales. *New Phytologist* **207**: 1170–1180.

Carlquist S. 1999. Wood, stem, and root anatomy of Basellaceae with relation to habit, systematics, and cambial variants. *Flora* **194**: 1–12.

Carlquist S. 2001. *Comparative wood anatomy. systematic, ecological and evolutionary aspects of dicotyledon wood*. Berlin, Germany: Springer.

Carlquist S. 2007. Successive cambia in Aizoaceae: products and process. *Botanical Journal of the Linnean Society* **153**: 141–155.

Carlquist S. 2010. Caryophyllales: a key group for understanding wood anatomy character states and their evolution. *Botanical Journal of the Linnean Society* **164**: 342–393.

Cirillo C, De Micco V, Rouphael Y, Balzano A, Caputo R, De Pascale S. 2017. Morpho-anatomical and physiological traits of two *Bougainvillea* genotypes trained to two shapes under deficit irrigation. *Trees* **31**: 173–187.

Clarke C, Schlauer J, Moran J, Robinson A. 2018. Systematics and evolution of Nepenthes. In: Ellison A, Lubomír A, eds. *Carnivorous plants: physiology, ecology, and evolution*. Oxford, UK: Oxford University Press, 58–69.

Cunha Neto IL. (2023). Vascular variants in seed plants—a developmental perspective. *AoB PLANTS* **15**. doi: 10.1093/aobpla/plad036.

Cunha Neto IL, Pace MR, Angyalossy V. 2021. A new interpretation of the successive cambia of some Nyctaginaceae as interxylary phloem. *International Journal of Plant Sciences* **182**: 620–637.

Cunha Neto IL, Pace MR, Douglas NA, Nee MH, de Sá CFC, Moore MJ, Angyalossy V. 2020a. Diversity, distribution, development, and evolution of medullary bundles in Nyctaginaceae. *American Journal of Botany* **107**: 707–725.

Cunha Neto IL, Pace MR, Hernández-Gutiérrez R, Angyalossy V. 2022. Linking the evolution of development of stem vascular system in Nyctaginaceae and its correlation to habit and species diversification. *EvoDevo* **13**: 1–24.

Cunha Neto IL, Silva JP, Angyalossy V. 2020b. Anatomy of vegetative organs in *Allionia* (Nyctaginaceae), with emphasis on the vascular system. *Journal of the Botanical Research Institute of Texas* **15**: 373–394.

De Bary A. 1884. *Comparative anatomy of the vegetative organs of the phanerogams and ferns*. Oxford, UK: Clarendon Press.

DeBuhr LE. 1977. Sectional reclassification of *Drosera* subgenus *Ergaleium* (Droseraceae). *Australian Journal of Botany* **25**: 209–218.

Decombeix AL, Boura A, Tomescu AMF. 2019. Plant hydraulic architecture through time: lessons and questions on the evolution of vascular systems. *The IAWA Journal* **40**: 387–420.

Drummond AJ, Ho SYW, Phillips MJ, Rambaut A. 2006. Relaxed phylogenetics and dating with confidence. *PLoS Biology* **4**: 699–710.

Franco-Estrada D, Sánchez D, Terrazas T, Arias S. 2021. Phylogenetic analysis of *Peniocereus* (Cactaceae, Echinocereeae) based on five chloroplast DNA markers. *Revista Brasileira de Botanica* **44**: 903–916.

Gibson AC. 1976. Vascular organization of shoots of Cactaceae. 1. Development and morphology of primary vasculature in Pereskioideae and Opuntioideae. *American Journal of Botany* **63**: 414–426.

Gibson AC. 1994. Vascular tissues. In: Behnke H-D, Mabry TJ, eds. *Caryophyllales. Evolution and systematics*. Berlin, Germany: Springer, 45–74.

Gibson AC, Nobel PS. 1986. *The cactus primer*. Cambridge, MA, USA: Harvard University Press.

Grigore MN, Toma C. 2017. Successive (additional) cambia. In: Grigore MN, Toma C, eds. *Anatomical adaptations of halophytes: a review of classic literature and recent findings*. Cham, Switzerland: Springer, 273–323.

Haberlandt GFJ. 1914. *Physiological plant anatomy*. London, UK: Macmillan Co.

Hall TA. 1999. BioEdit: a user-friendly biological sequence alignment editor and analysis program for Windows 95/98/NT. *Nucleic Acids Symposium Series* **41**: 95–98.

Hearn DJ. 2009. Developmental patterns in anatomy are shared among separate evolutionary origins of stem succulent and storage root-bearing growth habits in Adenia (Passifloraceae). *American Journal of Botany* **96**: 1941–1956.

Hearn DJ. 2019. Turing-like mechanism in a stochastic reaction-diffusion model recreates three dimensional vascular patterning of plant stems. *PLoS ONE* **14**: 1–24.

Hernández-Ledesma P, Berendsohn WG, Borsch T, Von Mering S, Akhani H, Arias S, Castañeda-Noa I, Eggli U, Eriksson R, Flores-Olvera H *et al.* 2015. A taxonomic backbone for the global synthesis of species diversity in the angiosperm order Caryophyllales. *Willdenowia* **45**: 281–383.

Isnard S, Prosperi J, Wanke S, Wagner ST, Samain MS, Trueba S, Frenzke L, Neinhuis C, Rowe NP. 2012. Growth form evolution in Piperales and its relevance for understanding angiosperm diversification: an integrative approach combining plant architecture, anatomy, and biomechanics. *International Journal of Plant Sciences* **173**: 610–639.

Joshi AC. 1936. The anatomy of *Rumex* with special reference to the morphology of the internal bundles and the origin of the internal phloem in the Polygonaceae. *American Journal of Botany* **23**: 362–369.

Kirchoff BK, Fahn A. 1984. The primary vascular system and medullary bundle structure of *Phytolacca dioica* (Phytolaccaceae). *Canadian Journal of Botany* **62**: 2432–2440.

Lanfear R, Calcott B, Ho SYW, Guindon S. 2012. PartitionFinder: combined selection of partitioning schemes and substitution models for phylogenetic analyses. *Molecular Biology and Evolution* **29**: 1695–1701.

Lens F, Gleason SM, Bortolami G, Brodersen C, Delzon S, Jansen S. 2022. Functional xylem characteristics associated with drought-induced embolism in angiosperms. *New Phytologist* **236**: 2019–2036.

Loza-Cornejo S, Terrazas T. 2011. Morfo-anatomía de plántulas en especies de Pachycereeae: hasta cuándo son plántulas? *Boletín de la Sociedad Botánica de México* **88**: 1–13.

Macdougal DT. 1926. Growth and permeability of century-old cells. *The American Naturalist* **60**: 393–415.

Maddison WP, FitzJohn RG. 2015. The unsolved challenge to phylogenetic correlation tests for categorical characters. *Systematic Biology* **64**: 127–136.

Maddison WP, Maddison DR. 2019. *Mesquite: a modular system for evolutionary analysis*. v.3.6. [WWW document] URL http://www.mesquiteproject.org [accessed 15 September 2023].

Maheshwari P. 1929. Origin and development of the internal bundles in the stem of *Rumex crispus*. *Journal of the Indian Botanical Society* **8**: 89–117.

Maheshwari P, Singh B. 1942. On the internal bundles in the stem of *Rumex patientia* L. *Proceedings/Indian Academy of Sciences* **45**: 153–157.

Mauseth JD. 1993. Medullary bundles and the evolution of Cacti. *American Journal of Botany* **80**: 928–932.

Mauseth JD. 2004. The structure of photosynthetic succulent stems in plants other than Cacti. *International Journal of Plant Sciences* **165**: 1–9.

Mauseth JD. 2006. Structure–function relationships in highly modified shoots of Cactaceae. *Annals of Botany* **98**: 901–926.

Metcalfe CR, Chalk L. 1983. Anatomy of the dicotyledons. In: *Wood structure and conclusion of the general introduction*, vol. **2**. Oxford, UK: Clarendon Press.

Murphy B, Forest F, Barraclough T, Rosindell J, Bellot S, Cowan R, Golos M, Jebb M, Cheek M. 2020. A phylogenomic analysis of *Nepenthes* (Nepenthaceae). *Molecular Phylogenetics and Evolution* **144**: 106668.

Myśkow E, Gola EM, Tulik M. 2019. Continuity of procambium and anomalous cambium during formation of successive cambia in *Celosia argentea*. *Journal of Plant Growth Regulation* **38**: 1458–1466.

Pagel M. 1994. Detecting correlated evolution on phylogenies: a general method for the comparative analysis of discrete characters. *Proceedings of the Royal Society B* **255**: 37–45.

Pagel M. 1999. Inferring the historical patterns of biological evolution. *Nature* **401**: 877–884.

Pennell MW, Eastman JM, Slater GJ, Brown JW, Uyeda JC, FitzJohn RG, Alfaro ME, Harmon LJ. 2014. Geiger v.2.0: an expanded suite of methods for fitting macroevolutionary models to phylogenetic trees. *Bioinformatics* **30**: 2216–2218.

Pfeiffer H. 1926. *Das abnorme Dickenwachstum – Handbuch der Pflanzenanatomie, Band IX*. Berlin, Germany: Verlag von Gebrüder Borntraeger.

Philipson WR, Balfour EE. 1963. Vascular patterns in dicotyledons. *Botanical Review* **29**: 382–404.

Plummer M, Best N, Cowles K. 2006. CODA: convergence diagnosis and output analysis for MCMC. *R News* **6**: 7–11.

R Core Team. 2022. *R: a language and environment for statistical computing*. Vienna, Austria: R Foundation for Statistical Computing.

Rabosky DL. 2014. Automatic detection of key innovations, rate shifts, and diversity-dependence on phylogenetic trees. *PLoS ONE* **9**: e89543.

Rabosky DL. 2018. BAMM at the court of false equivalency: a response to Meyer and Wiens. *Evolution* **72**: 2246–2256.

Rabosky DL, Grundler M, Anderson C, Title P, Shi JJ, Brown JW, Huang H, Larson JG. 2014. BAMMtools: an R package for the analysis of evolutionary dynamics on phylogenetic trees. *Methods in Ecology and Evolution* **5**: 701–707.

Rambaut A, Suchard MA, Xie D, Drummond AJ. 2014. *Trace*. v.1.6. [WWW document] URL http://tree.bio.ed.ac.uk/software/tracer/ [accessed 15 September 2023].

Renner T, Specht CD. 2013. Inside the trap: gland morphologies, digestive enzymes, and the evolution of plant carnivory in the Caryophyllales. *Current Opinion in Plant Biology* **16**: 436–442.

Revell LJ. 2012. Phytools: an R package for phylogenetic comparative biology (and other things). *Methods in Ecology and Evolution* **3**: 217–223.

Rivadavia F, Kondo K, Kato M, Hasebe M. 2003. Phylogeny of the sundews, *Drosera* (Droseraceae), based on chloroplast rbcL and nuclear 18S ribosomal DNA sequences. *American Journal of Botany* **90**: 123–130.

Robert EMR, Schmitz N, Copini P, Gerkema E, Vergeldt FJ, Windt CW, Beeckman H, Koedam N, Van As H. 2014. Visualization of the stem water content of two genera with secondary phloem produced by successive cambia through magnetic resonance imaging (MRI). *Journal of Plant Hydraulics* **1**: e006.

Ronse De Craene LP. 2013. Reevaluation of the perianth and androecium in Caryophyllales: implications for flower evolution. *Plant Systematics and Evolution* **299**: 1599–1636.

Ronse de Craene LP. 2021. Gynoecium structure and development in core Caryophyllales: a matter of proportions. *Botanical Journal of the Linnean Society* **195**: 437–466.

Schwallier R, Gravendeel B, De Boer H, Nylinder S, Van Heuven BJ, Sieder A, Sumail S, Van Vugt R, Lens F. 2017. Evolution of wood anatomical characters in *Nepenthes* and close relatives of Caryophyllales. *Annals of Botany* **119**: 1179–1193.

Smith SA, Brown JW, Yang Y, Bruenn R, Drummond CP, Brockington SF, Walker JF, Last N, Douglas NA, Moore MJ. 2018. Disparity, diversity, and duplications in the Caryophyllales. *New Phytologist* **217**: 836–854.

Soffiatti P, Angyalossy V. 2003. Stem anatomy of *Cipocereus* (Cactaceae). *Bradleya* **21**: 39–48.

Soffiatti P, Angyalossy V. 2007. Anatomy of Brazilian Cereeae (subfamily Cactoideae, Cactaceae). *Acta Botânica Brasílica* **21**: 813–822.

Stamatakis A. 2014. RAxML v.8: a tool for phylogenetic analysis and post-analysis of large phylogenies. *Bioinformatics* **30**: 1312–1313.

Suissa JS, Friedman WE. 2022. Rapid diversification of vascular architecture underlies the Carboniferous fern radiation. *Proceedings of the Royal Society B: Biological Sciences* **289**: 20212209.

Sukhorukov AP, Mavrodiev EV, Struwig M, Nilova MV, Dzhalilova KK, Balandin SA, Erst A, Krinitsyna AA. 2015. One-seeded fruits in the core Caryophyllales: their origin and structural diversity. *PLoS ONE* **10**: 1–38.

Sukhorukov AP, Nilova MV, Kushunina M, Mazei Y, Klak C. 2023. Evolution of seed characters and of dispersal modes in Aizoaceae. *Frontiers in Plant Science* **14**: 1–23.

Sukhorukov AP, Nilova MV, Moore MJ, Bruenn R, Last N, Rossetto EFS, Douglas NA. 2021. Anatomical diversity and evolution of the anthocarp in Nyctaginaceae. *Botanical Journal of the Linnean Society* **196**: 21–52.

Terrazas Salgado T, Mauseth JD. 2002. Shoot anatomy and morphology. In: Nobel PS, ed. *Cacti: biology and uses*. Berkeley, CA, USA: University of California Press, 22–40.

Terrazas T, Arias S. 2002. Comparative stem anatomy in the subfamily Cactoideae. *Botanical Review* **68**: 444–473.

Terrazas T, Loza-Cornejo S. 2002. Phylogenetic relationships of Pachycereeae: a cladistic analysis based on anatomical-morphological data. In: Fleming TH, Valiente-Banuet A, eds. *Columnar cacti and their mutualists*. Tucson, AZ, USA: University of Arizona Press, 66–86.

Thompson JD, Higgins DG, Gibson TJ. 1994. CLUSTALW: improving the sensitivity of progressive multiple sequence alignment through sequence weighting, position-specific gap penalties and weight matrix choice. *Nucleic Acids Research* **22**: 4673–4680.

Timoneda A, Feng T, Sheehan H, Walker-Hale N, Pucker B, Lopez-Nieves S, Guo R, Brockington S. 2019. The evolution of betalain biosynthesis in Caryophyllales. *New Phytologist* **224**: 71–85.

Timonin AK. 2011. *Anomalous secondary thickening of the root and stem in Centrosperms: specific of morphofuntional plant evolution*. Moscow, Russia: KMK Press.

Tomescu AMF. 2021. The stele – a developmental perspective on the diversity and evolution of primary vascular architecture. *Biological Reviews* **96**: 1263–1283.

Tyree MT, Ewers FW. 1991. The hydraulic architecture of trees and other woody plants. *New Phytologist* **119**: 345–360.

Walker JF, Yang Y, Feng T, Timoneda A, Mikenas J, Hutchison V, Edwards C, Wang N, Ahluwalia S, Olivieri J *et al.* 2018. From cacti to carnivores: improved phylotranscriptomic sampling and hierarchical homology inference provide further insight into the evolution of Caryophyllales. *American Journal of Botany* **105**: 446–462.

Wilson CL. 1924. Medullary bundle in relation to primary vascular system in Chenopodiaceae and Amaranthaceae. *Botanical Gazette* **78**: 175–199.

Yang Y, Moore MJ, Brockington SF, Mikenas J, Olivieri J, Walker JF, Smith SA. 2018. Improved transcriptome sampling pinpoints 26 ancient and more recent polyploidy events in Caryophyllales, including two allopolyploidy events. *New Phytologist* **217**: 855–870.

Yang Y, Moore MJ, Brockington SF, Soltis DE, Wong GK-S, Carpenter EJ, Zhang Y, Chen L, Yan Z, Xie Y *et al.* 2015. Dissecting molecular evolution in the highly diverse plant clade Caryophyllales using transcriptome sequencing. *Molecular Biology and Evolution* **32**: 2001–2014.

Yao G, Jin J-J, Li H-T, Yang J-B, Mandala VS, Croley M, Mostow R, Douglas NA, Chase MW, Christenhusz MJM *et al.* 2019. Plastid phylogenomic insights into the evolution of Caryophyllales. *Molecular Phylogenetics and Evolution* **134**: 74–86.

Zimmermann MH, Jeje A. 1981. Vessel-length distribution in stems of some American woody plants. *Canadian Journal of Botany* **59**: 1882–1892.

Zumaya-Mendoza S, Aguilar-Rodríguez S, Yáñez-Espinosa L, Terrazas T. 2019. Stem anatomy diversity in *Iresine* (Amaranthaceae sl): an ecological interpretation. *Revista Brasileira de Botanica* **42**: 329–344.

Supporting Information

Additional Supporting Information may be found online in the Supporting Information section at the end of the article.

Dataset S1 Beast-derived maximum clade credibility phylogenetic tree in nexus file format.

Dataset S2 Chronogram from BEAST analysis.

Dataset S3 List of taxa for Pagel's (1994) test of correlated evolution.

Fig. S1 Experiment 1 – hydraulic conductivity in *Bougainvillea spectabilis*.

Fig. S2 Experiment 1 – hydraulic conductivity in plants *Mirabilis jalapa*.

Fig. S3 Light microscopy images of stems from different species with regular eustele and polycyclic eustele (with medullary bundles) in Caryophyllales.

Fig. S4 Drawings of cross sections illustrating the diversity in number and arrangements of medullary bundles in Caryophyllales.

Fig. S5 Net diversification rates of medullary bundles using MEDUSA.

Methods S1 Data collection and histological procedures.

Methods S2 Phylogeny overview and topology comparisons.

Methods S3 Divergence time estimation.

Table S1 List of studied species with information on the presence/absence of medullary bundles and other types of conducting vascular tissue in the pith.

Table S2 Information of DNA partitions for Caryophyllales phylogeny.

Table S3 Dataset used for BAMM analysis and ancestral state reconstruction.

Table S4 Model comparisons for character evolution and branch transformation.

Table S5 Pagel's (1994) test of correlated evolution results.

Table S6 Model comparison from the trait-dependent diversification analysis.

Table S7 Measurements and summary statistics of hydraulic conductivity experiments.

Please note: Wiley is not responsible for the content or functionality of any Supporting Information supplied by the authors. Any queries (other than missing material) should be directed to the *New Phytologist* Central Office.